Research Article **Open Access**

Ernesto Amores*, Jesús Rodríguez, José Oviedo, and Antonio de Lucas-Consuegra

Development of an operation strategy for hydrogen production using solar PV energy based on fluid dynamic aspects

DOI 10.1515/eng-2017-0020
Received July 20, 2016; accepted April 25, 2017

Abstract: Alkaline water electrolysis powered by renewable energy sources is one of the most promising strategies for environmentally friendly hydrogen production. However, wind and solar energy sources are highly dependent on weather conditions. As a result, power fluctuations affect the electrolyzer and cause several negative effects. Considering these limiting effects which reduce the water electrolysis efficiency, a novel operation strategy is proposed in this study. It is based on pumping the electrolyte according to the current density supplied by a solar PV module, in order to achieve the suitable fluid dynamics conditions in an electrolysis cell. To this aim, a mathematical model including the influence of electrode-membrane distance, temperature and electrolyte flow rate has been developed and used as optimization tool. The obtained results confirm the convenience of the selected strategy, especially when the electrolyzer is powered by renewable energies.

Keywords: hydrogen production, alkaline water electrolysis, modelling, polarization curve, renewable energy, energy storage, fluid dynamic conditions

1 Introduction

The cost and availability of fossil fuels, the greenhouse gas emissions and the increasing energy demand are some of the most important problems which characterize the actual energy and transportation system. In contrast to the problems associated with fossil fuels, the renewable energy sources (RES) represent one of the most promising and sustainable alternatives for a change in the global energetic model. However its inherent dependence on weather conditions causes them to be intermittent and so adequate energy storage technologies are required in order to improve the RES integration. On one hand, the surplus energy can be stored and accessed later during times of demand; on the other hand, they can stabilize and relieve the grid [1].

The energy can be stored using different methods. Batteries are one of the most common solutions. On the other hand, pumped storage and compressed air storage (CAES) techniques are well-known and have been in use for decades in some cases [1]. However, their storage capacity is in the range of hours or a few days. In this context, hydrogen offers a promising alternative. It is a chemical energy storage solution and can therefore store more energy per volume than potential energy storage systems. Excess of electricity produced by RES, can be converted into hydrogen, stored and, when needed, it can be reconverted into electricity and heat with fuel cells. Figure 1 shows an example of a system based on renewable energy sources using hydrogen as energy vector. The result is an emissions-free energy carrier.

Besides the energy vector for electricity and heat production, hydrogen can be injected into the natural gas grid, utilized as a raw material for the chemical industry and for the synthesis of various hydrocarbon fuels such as methane or methanol (via CO_2 hydrogenation reaction) or synthetic diesel and gasoline fuels (via Fischer-Tropsch reaction). Moreover, hydrogen can also be directly used in mobility (fuel cell electric vehicles) and in various portable applications [2–6].

Although hydrogen can be obtained by different ways, water electrolysis is probably one of the most environmentally friendly strategies, mainly when renewable energy sources are used (RES-H_2). Among the different electrol-

***Corresponding Author: Ernesto Amores:** Centro Nacional del Hidrógeno (CNH2). Prolongación Fernando El Santo s/n, 13500 Puertollano, Ciudad Real, Spain, E-mail: ernesto.amores@cnh2.es
Jesús Rodrıguez, José Oviedo: Centro Nacional del Hidrógeno (CNH2). Prolongación Fernando El Santo s/n, 13500 Puertollano, Ciudad Real, Spain
Antonio de Lucas-Consuegra: Facultad de Ciencias y Tecnologías Químicas, Dpto. de Ingeniería Química, Universidad de Castilla-La Mancha (UCLM). Avda. Camilo José Cela 10, 13005 Ciudad Real, Spain

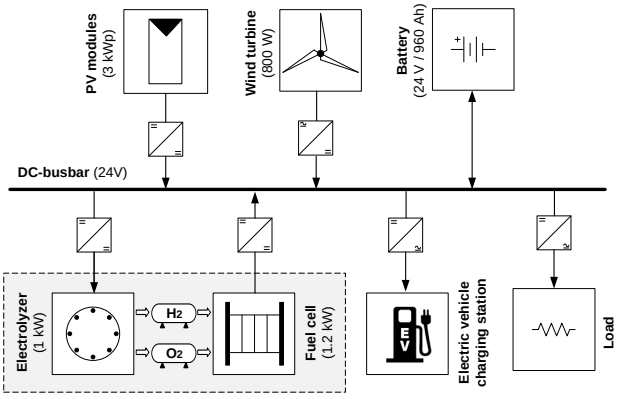

Figure 1: Example of a system based on renewable energy sources using hydrogen as an energy vector (adapted with permission from reference [6])

ysis technologies, the alkaline water electrolysis (AWE) is optimal for large scale hydrogen production because it is an economic and mature technology [1, 7]. However, wind and solar energy sources are highly dependent on weather conditions. As a result, power fluctuations affect the electrolyzer and cause several negative effects such as generation of explosive mixtures, corrosion materials problems, pressure drops and an increase on the electrolysis potential, among many others. Also, the high presence of bubbles in the anodic and cathodic compartments as consequence of gas generated during electrolysis increases the ohmic drops, especially under high current densities and small distances between the electrodes. It causes a growing energy demand on the electrolysis cells and lower overall process efficiency [8, 9].

There are several ways to reduce the gas fraction and improve the cell efficiency, such as different conditions gravity, ultrasound applications or magnetic fields [10]. However, a suitable and simple approach could be the fluid dynamics process optimization using a pump to drive the flow. As a result, the gas flows out of the cell faster. This strategy could be especially suitable for the typical power supply fluctuations of RES, because one could determine the optimal electrolyte flow rate depending of the solar irradiation or wind velocity, i.e. according to the amount of gas present in the cell.

In this context, the mathematical modelling can be a useful strategy in order to achieve a proper operation of alkaline electrolyzers powered by RES. One of the most detailed solar-hydrogen model was developed in the Fraunhofer Institute by Griesshaber and Sick [11] and later validated by Mørner [12]. Afterwards, Ulleberg [7] reported in 2003 a dynamic model for an alkaline electrolyzer, taking as reference these previous works. The model is based on a combination of fundamental thermodynamics, heat transfer theory and empirical relationships, and it is able to simulate the dynamic performance of an alkaline electrolyzer. In addition, this model has been frequently used for dynamic simulation of RES-H_2 systems because of its accuracy and adaptability to different electrolyzers [13]. It has also been used to improve process efficiency, evaluate economic performance or maximize the hydrogen production [14–19], among others. However, although this model accurately reproduces the polarization curve of an alkaline electrolysis cell, it does not include some others important operation parameters which can strongly influence in the electrolytic process. A later work reported the modification of this model which includes the influence of electrolyte concentration and the electrode-membrane distance [13].

The present work go a step forward and reports a new variation of the Ulleberg model, including the influence of the electrolyte flow, electrode-membrane distance, temperature and the applied current density. Using this model and the experimental results obtained about the fluid dynamics aspects of an electrolysis cell, the optimal flow rate can be calculated according to the current density.

In this way, it can establish an operating strategy for hydrogen production when an electrolyzer is powered by PV solar energy, by using the optimal flow rate conditions for each electric current value to minimize the energetic consumption of the electrolysis cell in each moment. The obtained model was experimentally validated reporting a low average error.

2 Hydrogen production by alkaline water electrolysis

Alkaline water electrolysis is the decomposition of water into hydrogen and oxygen by passing an electric current (DC) between two electrodes separated by a high ionic conductivity electrolyte (usually 30–35 wt% KOH aqueous solution). The theoretical fundamentals that explain this process are thermodynamics, kinetics of the reactions that occur at the electrodes and various transport phenomena involved in the electrolysis [7, 20]. The overall reaction for water splitting is shown in Equation (1):

$$H_2O \rightarrow H_2 + \frac{1}{2}O_2 \quad (1)$$

For this reaction to occur a minimum voltage is required, which is known as reversible voltage (U_{rev}), corresponding to 1.23 V [1] at standard conditions (1 bar and 25 °C). This value can be obtained from the second law of ther-

modynamics and the Gibbs free energy ($\Delta G°$= 273.2 kJ/mol in standard conditions).

However, the real cell voltage (U) is always higher than theoretical one because of irreversibilities. So, the real cell voltage can be defined as the sum of reversible voltage and overpotentials (η), as shown in Equation (2):

$$U = U_{rev} + \sum \eta \quad (2)$$

The term η is the sum of activation, ohmic and concentration overpotentials. These overpotentials are caused by [13, 21]:

- *Activation Overpotentials:* Related to activation energies of hydrogen and oxygen formation reactions on the surface of electrodes.
- *Ohmic Overpotentials:* Sum of the electrical resistance of some components like electrodes, current collectors, etc.; and the transport resistance related to gas bubbles, ionic transfer in the electrolyte and resistivity of membrane.
- *Concentration Overpotentials:* It is due to mass-transport limitations occurring on the surface of electrodes at high currents.

These overpotentials can be analysed through the polarization curve of an electrolysis cell, as shown in Figure 2. The curve models the reaction kinetics of water electrolysis and establishes the most appropriate values of voltage and current density. Usually, alkaline electrolysis cells operate between 400 and 600 mA/cm^2 with a voltage around 2.0 V and temperatures of 60–80 °C. The specific energy consumption to produce hydrogen ranges from 4.1 to 4.5 kWh/Nm^3 H_2 at 450 mA/cm^2 [20].

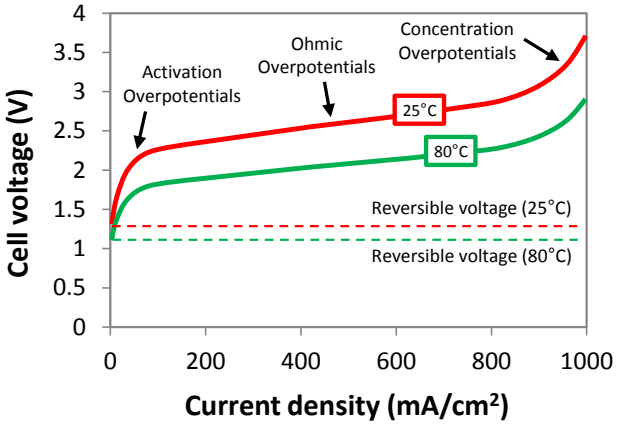

Figure 2: Polarization curve of an alkaline electrolysis cell at different temperatures.

3 Tests and experimental procedure

3.1 Alkaline electrolysis cell

Figure 3 shows a scheme of the alkaline electrolysis cell used in this study. The cell is filled with a 32 wt% KOH aqueous solution (electrolyte), where the hydroxyl ions (OH^-) are responsible for ion transport. Inside the cell are the electrodes, which are separated by a membrane or diaphragm that allows the flow of ions but it is impermeable to gases. All experiments were carried out under atmospheric pressure using Ni200 anode and SS316 cathode supplied by ElectroCell A/S. The active area for both electrodes was 10 cm^2. The diaphragm used was Zirfon® Perl 500 UTP supplied by AGFA.

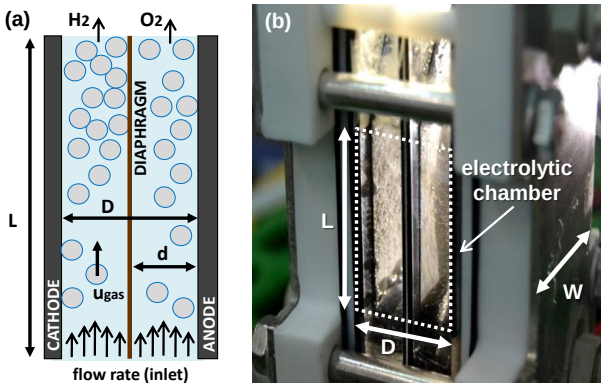

Figure 3: Alkaline electrolysis cell: (a) scheme, (b) detail image of the cell used in this study.

According to reaction show in Equation (1), oxygen bubbles are produced at the anode and hydrogen is produced at the cathode. These bubbles grow until they leave the electrode surface and rise up out of the electrolysis cell. The amount of generated gas inside the cell is quantified by gas volumetric fraction which is defined as the ratio between the generated gas volume and the electrolytic chamber volume. The gas volumetric fraction must be small in order to minimize the ohmic overpotentials on the cell.

3.2 Experimental procedure

The experiments were carried out in the alkaline water electrolysis facility schematized in Figure 4 [13], located in one of the laboratories of *Centro Nacional del Hidrógeno* (www.cnh2.es). The system has three electrolysis cells in

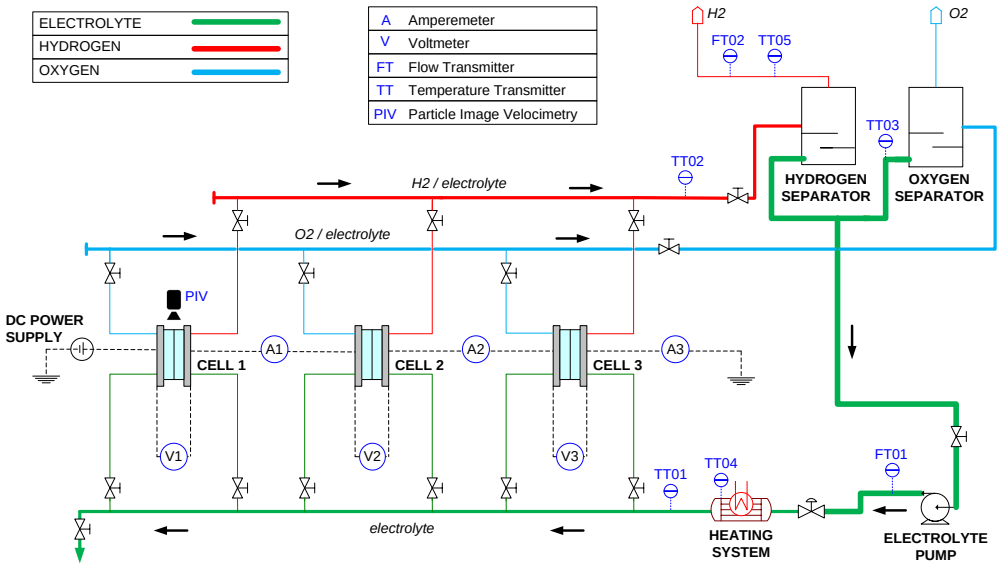

Figure 4: Alkaline electrolysis experimental facility used in this study.

series (ELECTROCELL, Micro Flow Cell), a DC power supply (Elektro-Automatik, EA-PSI 6000), a centrifugal magnetic drive pump (Plastomec, P-031-P), two separators for oxygen and hydrogen and a heating system (Hillesheim, H300 DN12) to adjust the temperature of the electrolyte. Also, the facility has different measurement and control devices which are monitored by a SCADA system (Supervisory Control and Data Acquisition) developed by means of NI LabVIEW software. Different PV profiles can be simulated by the DC power supply.

In the present study different flow rates (natural convection, 0.7, 1.4, 2.1 and 2.8 l/min), temperatures (30, 40, 50, 60 and 70 °C) and electrode-membrane distances (10, 4, 1.5 and 0.9 mm thickness frame) were tested according to an experimental central composite design [22]. In a typical test, once the electrode-membrane distance was fixed, the pump turned on to homogeneously distribute the electrolyte throughout the hydraulic circuit at the defined flow rate. Then, the heating system was activated. When the temperature was stable, the power supply was turned on, providing the required current to the cells to carry out the polarization curves. For each current value, different operation parameters were monitored and registered.

4 Empirical alkaline electrolyzer polarization curve fitting equation

The modelling is a useful tool to study the performance of an alkaline electrolyzer, especially when it is powered by renewable energies. As previously discussed, one of the most detailed models was proposed by Ulleberg [7] which provides a basic form of the polarization curve (i-U) for a given operation temperature:

$$U = U_{rev} + r \cdot i + s \cdot \log(t \cdot i + 1) \quad (3)$$

According to Equation (3), it can be observed that the voltage "U" (V) needed for the electrolysis at a specific electric current density "i" (mA/cm^2) results from the sum of three different terms [7]: reversible voltage (U_{rev}), ohmic overpotentials (second term of the equation) and activation overpotentials (third term). The influence of these overpotentials are taken into account by introducing the coefficients "t" (m^2/A) and "s" (V) correlated with activation overpotentials and "r" (Ωm^2) which corresponds to ohmic overpotentials. These parameters are defined in the next subsection. The term "s" is assumed as constant.

However, the mathematical model proposed by Ulleberg considers the temperature as the only operational variable, assuming others parameters as constants, such as the electrolyte flow rate or the distance between electrodes. These variables were studied individually by others authors, demonstrating their great influence on the fluid dynamics electrolysis [9, 13, 23, 24]. In this way,

some authors observed that forced convection improves the process because it reduces mass transfer limitations and favours the bubbles transport [23, 25, 26]. Also, other authors showed that the distance between the electrodes is strongly related to the behaviour of biphasic mixtures inside the cell and hence with the efficiency [8, 9, 13, 24].

In order to obtain a model which considers the influence of the electrode-membrane distance (d) and the electrolyte flow rate ($\dot{Q}$), two new parameters were incorporated into Equation (3): "q" ($\Omega\,m^2$) and "z" ($\Omega\,m^2$), respectively. Since both parameters have influence on the ohmic overpotentials, they may be added to the resistive term. Thus the new Equation (4) was proposed:

$$U = U_{rev} + (r + q + z) \cdot i + s \cdot \log(t \cdot i + 1) \tag{4}$$

In order to determine these parameters and to analyse their influence on the electrolysis cell, different experiments were carried out in the experimental facility shown in Figure 4. In the following subsections the main results are shown.

4.1 Influence of the temperature

The temperature is one of the most important operating parameters in the electrolysis (see Figure 2). When the operating temperature of the electrolysis cell increases, less electricity is required because the free reaction enthalpy decrease and the overall kinetics and the ionic conductivity of the electrolyte increase [13, 20]. According to the model proposed by Ulleberg [7], the influence of temperature (T) can be determined by Equations (5) and (6):

$$r = r_1 + r_2 \cdot T \tag{5}$$

$$t = t_1 + \frac{t_2}{T} + \frac{t_3}{T^2} \tag{6}$$

The ohmic resistance coefficient "r" shows a linear temperature dependence, while "t" presents a quadratic performance [7]. On the other hand, "r_1", "r_2", "t_1", "t_2" and "t_3" are constants which can be obtained from experimental data.

4.2 Influence of the electrode-membrane distance

The ohmic losses depend on the distance between electrode and membrane (i.e. the electrolytic chamber volume). This is especially relevant at high current densities and low flow rates due to the low removal rate of the produced bubbles. Figure 5a shows the polarization curve when different electrode-membrane distances were used in natural convection operation mode [22]. It was noted that when the distance was reduced from 10 mm to 1.5 mm, the required potential for the electrolysis always decreased because the electrolyte conductivity increased. But, when the distance continued to shrink up to 0.9 mm in the tests performed in this study, the voltage increased to similar values to those observed at a distance of 4 mm. However, when forced convection was used (in this case 0.7 l/min), the voltage is always reduced when the distance decreased (Figure 5b).

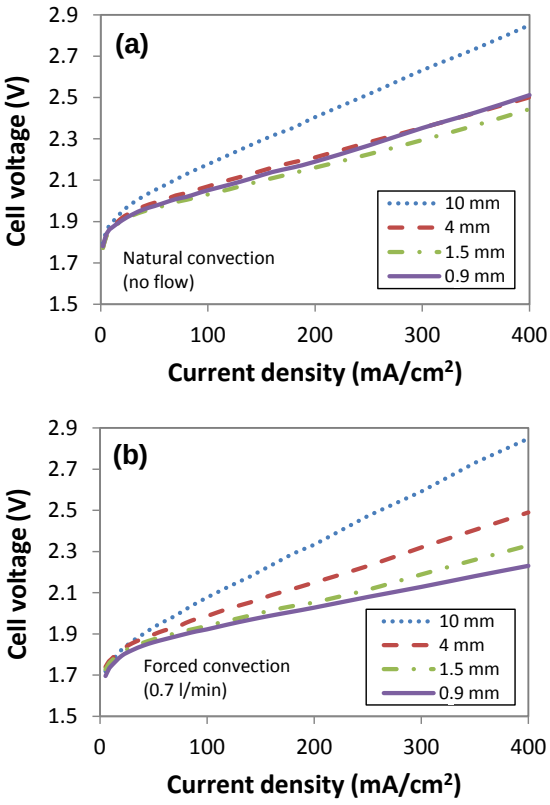

Figure 5: Polarization curve at different electrode-membrane distances and electrolyte flow rates: (a) natural convection, (b) 0.7 l/min [22].

These results suggest that there is an optimum electrode-membrane distance that may vary with the flow [8]. Nagai et al. [9, 24] obtained a theoretical equation to calculate the optimal distance between membrane and electrode (d_{opt}) of an electrolysis cell, according to the temperature (T), height electrode (L), pressure (p), Faradays' constant (F), universal gas constant (R) and rise of

gas bubbles (u_{gas}):

$$d_{opt}=\frac{1}{2}\cdot\left(1.271\cdot\frac{R\cdot L}{F\cdot p}\cdot\frac{T}{u_{gas}}\cdot i\right) \quad (7)$$

Using Equation (7) the optimal distance at natural convection in this study was equal to 2.19 mm at 400 mA/cm^2 (50 °C, electrode height 33 mm and 101325 Pa). But when experimental data were used, the optimum in these conditions was equal to 2.30 mm, so the values obtained with the Equation (7) are slightly lower than those obtained experimentally (Figure 8a). However, the theoretical values allow establishing a good approximation of the optimal distance. Then, using Equation (7) and according to the experimental results, the following equation was proposed to more accurately model the effect of distance (d) on the ohmic overpotentials:

$$q = q_1 + q_2\cdot|d - d_{opt}| \quad (8)$$

Equation (8) shows a lineal relation between electrode-membrane distance (d) with the potential required in the electrolysis through the constants "q_1" and "q_2". If the distance is greater than optimal distance ($d > d_{opt}$), the potential decreases when the electrode-membrane distance reduces (Figure 8a). But, if the distance is lower than the d_{opt}, the potential increases because the produced gas is confined in the vicinity of the electrode, when natural convection is used (Figure 8a).

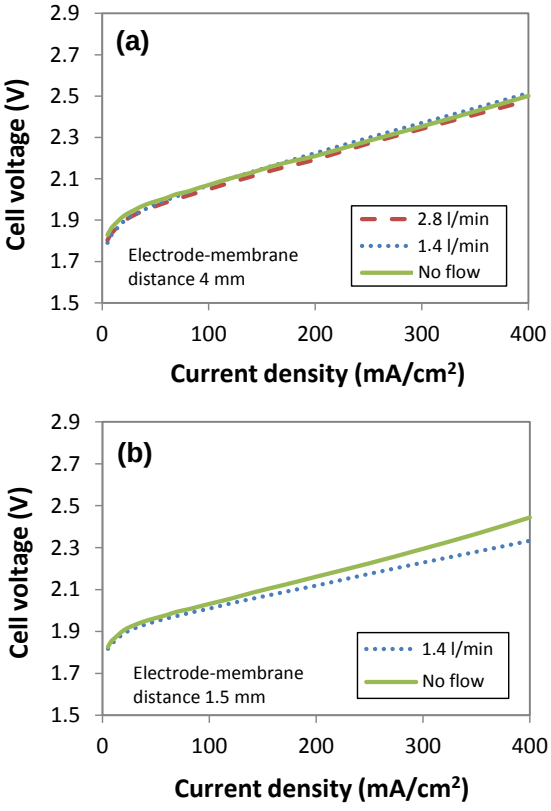

Figure 6: Polarization curve at different electrolyte flow rates and distances: (a) 4 mm, (b) 1.5 mm [22].

4.3 Influence of the electrolyte flow rate

In order to analyse the influence of the forced convection, experiments at different electrolyte flow rates ($\dot{Q}$) were carried out. The experimental data showed that when electrode-membrane distance was large (4 and 10 mm), the polarization curve was always the same regardless the flow rate (Figure 6a). This showed that under these conditions the forced convection did not have any influence on the electrical potential required for the electrolysis. However, when small electrode-membrane distances were used (0.9 and 1.5 mm), forced convection improved the efficiency by reducing bubbles ohmic overpotentials (Figure 6b) until a certain flow rate was reached. Above this specific value, no significant improvements were further observed (Figure 8b).

According to Takeuchi et al. [25] forced convection clearly affects the efficiency of water electrolysis: when flow velocity becomes larger, the efficiency of water electrolysis becomes higher. This effect is higher when density current rises because at low electrode-membrane distances the electrolytic cell volume is very limited, so the

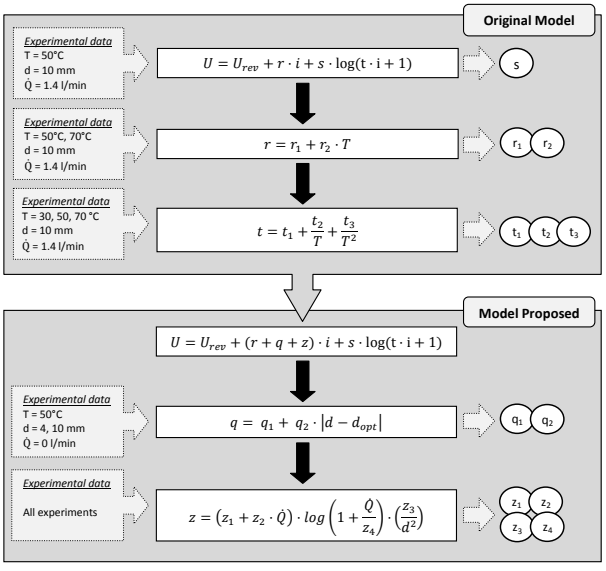

Figure 7: Procedure used to determine the coefficients of the mathematical model proposed.

gas completely fills the entire space during electrolysis. In these conditions, forced convection can quickly remove

the bubbles inside the cell. However in cells with larger distance between the electrodes, the gas can be effectively distributed by a greater amount of volume, so new electrolyte may continuously reach the electrodes.

In order to model the performance described above, the Equation (9) were proposed in this work:

$$z = (z_1 + z_2 \cdot \dot{Q}) \cdot \log\left(1 + \frac{\dot{Q}}{z_4}\right) \cdot \frac{z_3}{d^2} \quad (9)$$

In Equation (9) the constants "z_1", "z_2", "z_3" and "z_4" represent the influence of electrolyte flow rate and the electrode-membrane distance in the ohmic overpotentials. The term $(z_1 + z_2 \cdot \dot{Q})$ reproduces the reduction of voltage required when electrolyte flow increases. The term $\log(1 + \dot{Q}/z_4)$ mitigates the effect of forced convection at high flow rates and overrides the Equation (9) if natural convection is used because the parameter "z" is zero, so the ohmic overpotentials would be defined only by "r" and "q". Finally z_3/d^2 indicates that the electrolyte flow has a lower effect in the potential when distance between the electrodes is higher than a certain value.

5 Operation strategy proposed

5.1 Resolution of the model

The results obtained in this study showed that the temperature, the electrolyte flow rate and the electrode-membrane distance are closely related to each other and they have a clear influence on the ohmic overpotentials in the electrolysis, especially at high current densities. The mathematical model presented in Equation (4) reproduces these effects and so it is a useful tool to predict the polarization curve of an electrolyzer. Therefore, rearranging Equations (5), (6), (8) and (9) in Equation (4), the complete model equation is shown below:

$$U = U_{rev} + \left[r_1 + r_2 \cdot T + q_1 + q_2 \cdot |d - d_{opt}| + (z_1 + z_2 \cdot \dot{Q}) \cdot \log\left(1 + \frac{\dot{Q}}{z_4}\right) \cdot \frac{z_3}{d^2}\right] \cdot i + s \cdot \log\left[\left(t_1 + \frac{t_2}{T} + \frac{t_3}{T^2}\right) \cdot i + 1\right] \quad (10)$$

Table 1 contains the constants used for the modelling. The MATLAB software "Non Linear Model" class was used in order to determine these coefficients. This class allows doing a non-linear regression from constants of Equation (10), taking as input data the potential (V) and the current density (mA/cm^2) from each experiment, according to the procedure shown on Figure 7 and based on the methodology described in reference [13].

5.2 Optimal flow rate

The input variables in Equation (10) are temperature, electrode-membrane distance, electrolyte flow rate and current density. However, in an alkaline electrolysis cell, the electrode-membrane distance is an initial design parameter, previously set during the assembly of the electrolyzer. So, this distance cannot be changed afterwards the electrolyzer is manufactured. On the other hand, the operating temperature is usually 60–80 °C. Therefore, current density and flow rate are the only variables to consider, once the rest of the parameters are fixed. Since the current varies depending on the power supply used (for example, the electrical current provided by a PV panel along a day), the key parameter to be adjusted to optimize the process is the electrolyte flow rate.

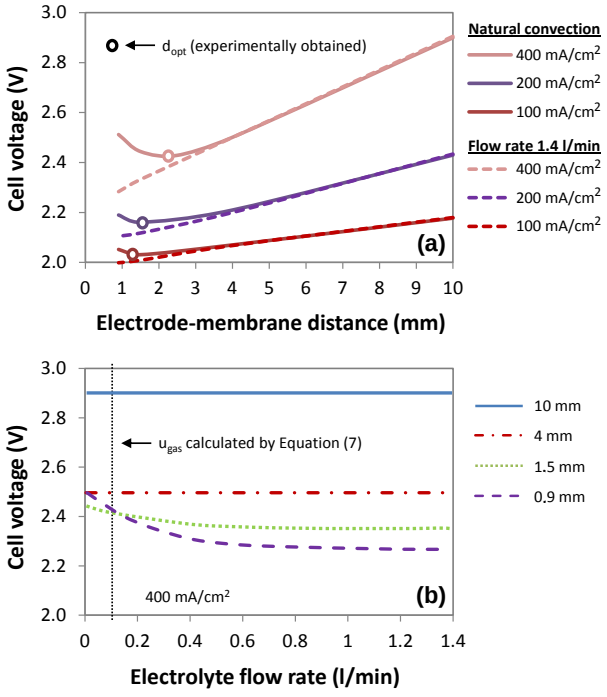

Figure 8: Cell voltage at 50°C and different experimental conditions: (a) with different electrode-membrane distances; (b) with different electrolyte flow rates.

According to the experimental data obtained in this study, forced convection generally improves the efficiency of the electrolysis process. However, a higher pumping flow requires an increasing amount of energy supplied and hence an overall reduction of the global efficiency of the system. Then, according to our study, a suitable method to reduce pumping energy requirements is to optimize the pump operation by controlling the electrolyte

Table 1: Coefficients obtained for the polarization curve model.

Coefficients		Value	Unit
Original model proposed by Ulleberg	r_1	0.000329491987	$\Omega \cdot m^2$
	r_2	−0.000002153281	$\Omega \cdot m^2 \cdot °C^{-1}$
	s	0.100601624017	V
	t_1	114609.51	$m^2 \cdot A^{-1}$
	t_2	−12397438.71	$m^2 \cdot °C \cdot A^{-1}$
	t_3	409431775.52	$m^2 \cdot °C^2 \cdot A^{-1}$
Model proposed in this study (coefficients added to the original model)	q_1	−0.000131093326	$\Omega \cdot m^2$
	q_2	0.000017739286	$\Omega \cdot m^2 \cdot mm^{-1}$
	z_1	−0.730	$\Omega \cdot m^2$
	z_2	−1.462	$\Omega \cdot m^2 \cdot min \cdot l^{-1}$
	z_3	0.000075	mm^2
	z_4	1.000	$l \cdot min^{-1}$

flow depending of the current density applied to the electrolyzer. This approach fit very well with the typical power supply fluctuations of RES, because one could determine the optimal electrolyte flow conditions depending on the solar irradiation or wind velocity available at that time.

Figure 8 shows the experimental results when the effect of the electrode-membrane distance and the flow rate are combined in order to analyse both effects at the same time on the cell voltage. Figure 8a shows that if electrode-membrane distance is large ($d > d_{opt}$), there is no advantage when forced convection is used. In this situation, it is never necessary to pump the electrolyte. However, when electrode-membrane distance is small ($d < d_{opt}$) and natural convection is used, the voltage required for electrolysis increases. But if a high enough flow rate value is applied the potential always diminishes (in this case 1.4 l/min). Figure 8b shows this effect in a large range of electrolyte flow rates: for large distances the flow never has an effect on the voltage; however, when the distance is small, an increase of flow rate reduces the voltage until reaching a flow rate value, beyond which, any increase does not produce any significant improvements in the electrolysis.

Based on the results shown in Figure 8, an optimal flow rate can be proposed ($\dot{Q}_{opt}$) in order to minimize the voltage required by the electrolysis at each current value, using a pump that drives the electrolyte. In this way, the energy consumption by the electrolysis cell can be optimized as follows in order to use only the exact flow rate at any time as shown in Equation (11):

$$\dot{Q}_{opt} \begin{cases} \text{when } d \geq d_{opt} \Rightarrow & \\ = 0\ l/min & \text{in all cases} \\ \text{when } d < d_{opt} \Rightarrow & \\ = 0\ l/min & \text{if } u_{St} \geq u_{gas,\,opt} \\ = 2Wd\varphi(u_{gas,\,opt} - u_{St}) & \text{if } u_{St} < u_{gas,\,opt} \end{cases} \tag{11}$$

Where "d_{opt}" is calculated by Equation (7), "W" is the width of the cell and "φ" is an adimensional parameter obtained experimentally from Figure 8. This parameter indicates how much the flow rate must be increased when the electrode-membrane distance is small. On the other hand, the Stokes velocity (u_{St}) is the terminal velocity at which a bubble of density "ρ_g" and diameter "$\emptyset_g$" will rise in a medium (30–35 wt% KOH) of density "ρ_L" and dynamic viscosity "μ_L" [23]. The Stokes velocity is therefore the gas velocity in natural convection and it does not depend on the current density or cell size:

$$u_{St} = \frac{1}{18} \cdot g \cdot \emptyset_g^2 \cdot \frac{\rho_L - \rho_g}{\mu_L} \tag{12}$$

Finally, "$u_{gas,opt}$" can be calculated by rewriting the Equation (7), when the considered distance correspond to the real electrode-membrane one, once the electrolysis cell has been assembled. In this way, the gas velocity will be proportional exclusively to the current density. Figure 9 shows the theoretical rise gas for the electrode-membrane distances used in this study at different current densities. In a dotted line is shown the rise velocity calculated using Equation (12), i.e. the gas velocity in natural convection when there is not a forced flow that impels the electrolyte and bubbles rise only by the balance of forces between buoyancy and drag (around 1.05 cm/s in this study).

According to Figure 9, when the distance is 10 mm or 4 mm, the Stokes velocity is enough to maintain optimum flowing conditions for any current density ($u_{St} > u_{gas,opt}$) avoiding the pumping of the electrolyte. This fact justified the results reported in Figure 8. However, when the electrode-membrane distance is 1.5 mm, forced convection is required if the current density is 290 mA/cm^2 or higher, because a faster rise is needed. For 0.9 mm, forced convection is required when current density is higher than 180 mA/cm^2.

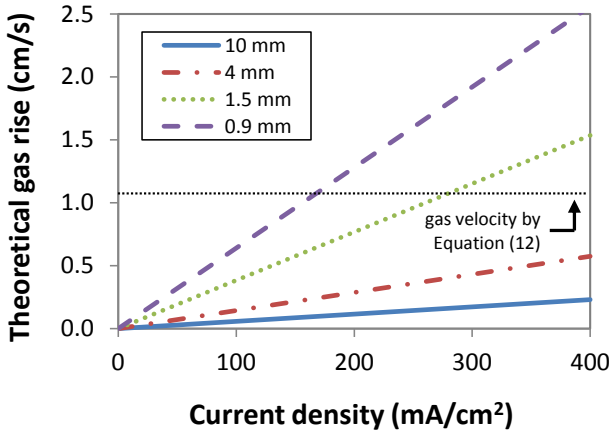

Figure 9: Theoretical gas rise at 50°C for different distances and current densities.

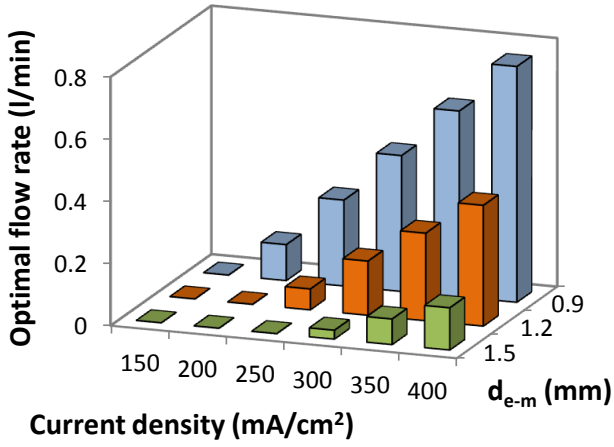

Figure 10: Optimal flow rate calculated in this study at 50°C for small electrode-membrane distances and different current densities.

Figure 10 shows the optimal flow rate calculated by Equation (11) for small electrode-membrane distances: 0.9, 1.2 and 1.5 mm. It is noted that when the current density is lower than 150 mA/cm^2 convection forced is not necessary in none of these cases. But if the current density increases, the required flow rate is higher, especially when the distance is getting smaller.

5.3 Optimized operation approach

With the goal of proposing an optimized operation approach, Equations (10) and (11) must be combined at each moment following this strategy:

- Firstly "$u_{gas,opt}$" is calculated using Equation (7) considering the real electrode-membrane distance (d) of the electrolysis cell for the whole range of electrical currents to model.
- Secondly "u_{St}" is obtained by Equation (12) with the properties of the biphasic mixture (density, viscosity and average bubble diameter, which in this study has been estimated at 180 µm).
- Later, "d_{opt}" is calculated by Equation (7) considering $u_{gas} = u_{St}$ for each electrical current to model.
- Then, with the data previously calculated ($u_{gas,opt}$, u_{St} and d_{opt}), the optimum flow rate is obtained ($\dot{Q}_{opt}$) for each value of current in the entire range to model according to Equation (11).
- Finally, entering the value of optimum flow rate ($\dot{Q}_{opt}$) in Equation (10) for each current density value, the minimum voltage can be obtained (at a constant d and T).

6 Results of the model and discussion

This section shows the model results corresponding to the interaction between electrolyte flow rate and electrolysis cell voltage when working with RES. To evaluate the model response using a renewable energy supply, a dynamic analysis was performed by applying a current profile corresponding to a photovoltaic panel, based on solar profiles in the city of Puertollano (Spain). In order to perform a wide evaluation, two different profiles were chosen (Figure 11):

- *A profile* corresponding *to a sunny day*, where the irradiance describes a parabola with minimum values at sunrise and sunset, and a maximum at solar midday.

– *A profile* corresponding *to a cloudy day*, with a considerable degree of irradiation variability, due to fluctuations at moments of high cloudiness.

In order to carry out tests using renewable energy sources, photovoltaic data profiles (Figure 11) were introduced in a SCADA program which controls the DC power supply. It supplies current to the cells, according to the considered solar profile. As shown in Figure 11 (right), the output current of the power supply was stepped as a result of discretization performed by the SCADA system.

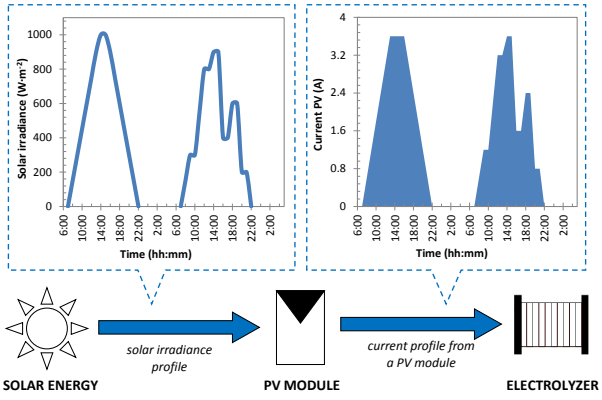

Figure 11: Solar profile and considered response of a PV panel along a sunny and a cloudy day [13].

Figure 12 shows the simulated performance of an alkaline water electrolysis cell in combination with RES, when it works with forced and natural convection for both PV profiles (sunny and cloudy) at 50°C and an electrode-membrane distance of 0.9 mm. For the case of the sunny day (Figure 12a), the efficiency of electrolysis process increases when the electrolyte is pumped, which can be clearly observed at higher current values (higher gas volumetric fraction). The effect of the forced convection when PV energy is applied during a cloudy day is reported in Figure 12b. Also in this case, the required potential for a high current value is lower when pump is activated. Moreover, it is observed than forced convection lightly reduced the typical fluctuations of a cloudy day PV profile, which could limit some negative effects related with RES combination as explosive mixture formation or materials degradation, among others.

On the other hand, the results reported in Figure 12 also show the convenience of the optimized strategy described in this study: when the flow rate is constant (for example 0.4 l/min), the potential is the same as in natural convection at low currents (sunrise and sunset). Therefore, the pumping of the electrolyte does not have any advantage in the electrolysis being on these cases the optimized flow null. However, when the current density is high, pumping flow is a useful strategy to reduce the overpotentials. Under this condition, using the optimal flow rate for each electric current value allows reaching the minimum potential for electrolysis at all times (Figure 12). In

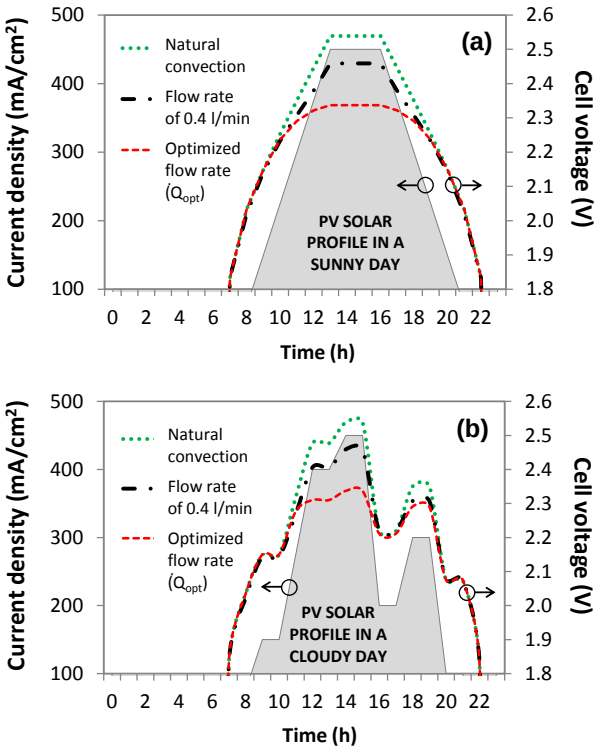

Figure 12: Cell voltage vs. time with respect to the proposed PV profile at different flow rates for: (a) sunny day, (b) cloudy day.

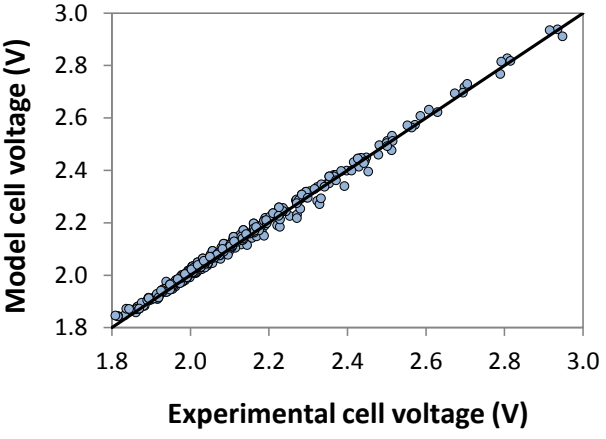

Figure 13: Parity chart of the model and experimental voltage results.

fact, at high current densities, the required flow is greater than 0.4 l/min.

Finally, in order to ensure the accuracy and validity of the proposed model, it was experimentally validated, obtaining an excellent correlation between the experimental and calculated results, as confirmed by the mean relative absolute difference (MRAD) error calculated according to Equation (13). The error was lower than 0.7%. Figure 13 shows a parity chart of the experimental and model cell voltage results used in this paper. Observed trends for the different operation parameters were consistent with other studies [1, 7, 20, 24].

$$MRAD\ error = \frac{1}{N}\sum_{i=1}^{N}\left|\frac{U_{model}-U_{exp}}{U_{exp}}\right| \quad (13)$$

7 Conclusions

The present study reports a mathematical model taking into account the influence of electrolyte flow, electrode-membrane distance, temperature and density current. The developed model is able to reproduce the polarization curve of an alkaline electrolysis cell under different operating conditions when it is powered by renewable energies. It is a semi-empirical model based on experimental data. Through this model, a methodology of operation can be established based on fluid dynamics aspects for hydrogen production varying the electrolyte flow rate, when the electrolyzer is powered by PV solar energy, in order to minimize the potential required in the electrolysis.

However, although in this study the positive effect of forced convection and the usefulness of the developed model are demonstrated, additional factors must be taken into account in order to analyse the proposed strategy. In the present study, only the energy consumption of the alkaline electrolysis cell is considered. Nevertheless, when a pump is used for pumping the electrolyte, more power is required in the entire process, so the overall energy consumption increases. This fact can limit the use of the pump, because it would start up at higher current values than those calculated in this work. To determine these values, a new economic and energy study should be performed to establish at what moment the reduction in the electrolysis potential compensates the increase of energy consumption of the pump when it is turned on.

Acknowledgement: The work described in this paper has been developed within the project *Experimentación, Simulación y Validación de Celdas de Electrólisis Alcalina para Producción de Hidrógeno mediante Energías Renovables* (EXSIVA) in the facilities of the Centro Nacional del Hidrógeno (CNH2) between 2014-2016, whose financial supporters are *Ministerio de Economía, Industria y Competitividad* (MINECO, Spain), *Junta de Comunidades de Castilla-La Mancha* (JCCM, Spain) and *European Regional Development Fund* (ERDF).

Nomenclature

AWE alkaline water electrolysis
CAES compressed air storage techniques
d electrode-membrane distance, [mm]
d_{opt} optimal electrode-membrane distance, [mm]
D electrode-electrode distance, [mm]
exp experimental
F Faraday constant, [96485 C/mol]
i current density, [mA/cm^2]
L height electrode, [mm]
MRAD mean relative absolute difference
p pressure, [Pa]
PV photovoltaic
q parameter related to ohmic resistance (electrode-membrane distance), [Ω·m^2]
$\dot{Q}$ electrolyte flow rate, [l/min]
$\dot{Q}_{opt}$ optimal electrolyte flow rate, [l/min]
r parameter related to ohmic resistance, [Ω·m^2]
R universal gas constant [8.314 J/(K·mol)]
RES renewable energy sources
s coefficient for overvoltage on electrodes, [V]
SCADA supervisory control and data acquisition
t coefficient for overvoltage on electrodes, [m^2/A]
T temperature, [°C]
u_{gas} bubble rising velocity, [mm/s]
$u_{gas,opt}$ optimal bubble rising velocity, [mm/s]
u_{St} Stokes velocity, [mm/s]
U voltage, [V]
U_{rev} reversible voltage, [V]
W width electrode, [mm]
z parameter related to ohmic resistance (electrolyte flow rate), [Ω·m^2]
η overpotentials, [V]
μ_L dynamic viscosity [Pa·s]
ρ density (kg/m^3)
φ adimensional parameter related to flow rate when distance is small
$\emptyset_g$ bubble diameter (mm)

References

[1] Töpler J., Lehmann J., Hydrogen and fuel cell – technologies and market perspectives, 1st ed., Springer-Verlag Berlin Heidelberg, Springer, 2016

[2] Ball M., Wietschel M., The future of hydrogen – opportunities and challenges, Int. J. Hydrogen Energy, 2009, 34(2), 615-627

[3] Pletcher D., Li X., Prospects for alkaline zero gap water electrolysers for hydrogen production, Int. J. Hydrogen Energy, 2011, 36(23), 15089-15104

[4] Ulleberg Ø., Nakken T., Eté A., The wind/hydrogen demonstration system at Utsira in Norway, Int. J. Hydrogen Energy, 2010, 35(5), 1841-1852

[5] Sánchez M., Manjavacas G., Olavarrieta J.M., Fúnez C., RENOVAGAS PROJECT: getting synthetic natural gas from renewable energy sources, In: 5^{th} Iberian Symposium on Hydrogen, Fuel Cells and Advanced Batteries (5-8 July 2015, Tenerife, Spain), University of La Laguna, 2015

[6] Hidalgo D., Martín J.J., Merino C., Almacenamiento de energía en ciclo de hidrógeno para sistemas aislados, In: Libro de Comunicaciones del 2^{nd} Congreso Smartgrids (27-28 October 2014, Madrid, Spain), Grupo Tecma Red, 2014, 95-99

[7] Ulleberg Ø., Modeling of advanced alkaline electrolyzers: a system a system simulation approach, Int. J. Hydrogen Energy, 2003, 28(1), 21-33

[8] Divisek J., Schmitz H., A bipolar cell for advanced alkaline water electrolysis, Int. J. Hydrogen Energy, 1982, 7(9), 703-710

[9] Nagai N., Takeuchi M., Nakao M., Influences of bubbles between electrodes onto efficiency of alkaline water electrolysis, In: Proceedings of 4th Pacific Symposium on Flow Visualization and Image (3-5 June 2003, Chamonix, France), Pacific Center of Thermal Fluids Engineering, 2003

[10] Mazloomi S. K., Sulaiman N., Influencing factors of water electrolysis electrical efficiency, Renewable and Sustainable Energy Reviews, 2012, 16(6), 4257-4263

[11] Griesshaber W., Sick F., Simulation des Wasserstoff-Sauerstoff-Systems mit PV-anlage für das energieautarke Solarhaus. Abteilung Systemtechnik/Simulation, Fraunhofer Institut für Solare Energiesysteme, Freiburg im Breisgau, 1991

[12] Mørner S.O., Seasonal storage of solar energy for self-sufficient buildings with focus on hydrogen systems, PhD thesis, Norwegian Institute of Technolgy, Trondheim, Norway, 1995

[13] Amores E., Rodríguez J., Carreras C., Influence of operation parameters in the modeling of alkaline water electrolyzers for hydrogen production, Int. J. Hydrogen Energy, 2014, 39(25), 13063-13078

[14] Diéguez P.M., Ursúa A., Sanchis P., Sopena C., Guelbenzu E., Gandía L.M., Thermal performance of a commercial alkaline water electrolyzer: Experimental study and mathematical modeling, Int. J. Hydrogen Energy, 2008, 33(24), 7338-7354

[15] Valenciaga F., Evangelista C.A., Control design for an autonomous wind based hydrogen production system, Int. J. Hydrogen Energy, 2010, 35(11), 5799-5807

[16] Đukić A., Firak M., Hydrogen production using alkaline electrolyzer and photovoltaic module, Int. J. Hydrogen Energy, 2011, 36(12), 7799-7806

[17] Carapelluci R., Giordano L., Modeling and optimization of an energy generation island based on renewable technologies and hydrogen storage systems, Int. J. Hydrogen Energy, 2012, 37(3), 2081-2093

[18] Mori M., Mrzljak T., Drobnič B., Sekavčnik M., Integral characteristics of hydrogen production in alkaline electrolysers, Strojniški vestnik - Journal of Mechanical Engineering, 2013, 59(10), 585-594

[19] Khalilnejad A., Riahy G.H., A hybrid wind-PV system performance investigation for the purpose of maximum hydrogen production and storage using advanced alkaline electrolyzer, Energ Convers Manage, 2014, 80, 398-406

[20] Gandía L.M., Arzamendi G., Diéguez P.M., Renewable hydrogen technologies: production, purification, storage, applications and safety, 1st ed., Elsevier BV, Elsevier, 2013

[21] Zeng K., Zhang D., Recent progress in alkaline water electrolysis for hydrogen production and applications, Prog Energy Combust Sci, 2010, 36(3), 307-326

[22] Amores E., Rodríguez J., Oviedo J., de Lucas-Consuegra A., Influence of fluid dynamic behavior in the ohmic overpotentials of an alkaline water electrolysis cell, In: Proceedings of 21^{st} World Hydrogen Energy Conference (13-16 June 2016, Zaragoza, Spain), Spanish Hydrogen Association, 2016, 910-912

[23] Schillings J., Doche O., Deseure J., Modeling of electrochemically generated bubbly flow under buoyancy-driven and forced convection, Int. J. of Heat and Mass Transfer, 2015, 85, 292-299

[24] Nagai N., Takeuchi M., Kimura T., Oka T., Existence of optimum space between electrodes on hydrogen production by water electrolysis, Int. J. Hydrogen Energy, 2003, 28, 35-41

[25] Takeuchi M., Furtua T., Efficiency and two-phase flow of alkaline water electrolysis under forced convection of electrolyte, In: Annals of the Assembly for 13^{rd} International Heat Transfer Conference (13-18 August 2006, Sydney, Australia), Begell House Inc, 2006

[26] Nagai N., Takeuchi M., Furtua T., Effects of bubbles between electrodes on alkaline water electrolysis efficiency under forced convection of electrolyte, In: Proceedings of 16^{th} World Hydrogen Energy Conference (13-16 June 2006, Lyon, France), Association Francaise pour l'Hydrogene et les Piles a Combustible, 2006, 100-109